

**RAMAN AND TIME GATED-LIF SPECTROSCOPY FOR THE IDENTIFICATION OF PAINTING MATERIALS \* \*\***

**M. Romani<sup>1\*</sup>, S. Almaviva<sup>2</sup>, F. Colao<sup>2</sup>, R. Fantoni<sup>2</sup>, M. Marinelli<sup>1</sup>,  
A. Pasqualucci<sup>1</sup>, A. Puiu<sup>2</sup>, G. Verona-Rinati<sup>1</sup>**

<sup>1</sup> INFN, Dipartimento di Ingegneria Industriale, Università degli studi di Roma “Tor Vergata”  
via del Politecnico 1, 00133, Rome, Italy; e-mail: [martina.romani@uniroma2.it](mailto:martina.romani@uniroma2.it)

<sup>2</sup> ENEA, Italian National Agency for New Technologies, Energy and Sustainable Economic Development,  
00044, Frascati, Rome, Italy

*A detailed characterization of painting materials by Raman and time gated laser induced fluorescence (TG-LIF) spectroscopy is proposed. The complementary capabilities of the considered techniques are investigated on a set of laboratory samples realized simulating real artworks. The achieved results confirmed the capability of Raman spectroscopy to characterize pigments and dyes, while the identification of binders and protective materials proved to be difficult because of their intense fluorescence. For this reason, the analyzed samples were also classified by TG-LIF spectroscopy in terms of their characteristic emission wavelengths and decay times. The complementary capabilities of Raman and TG-LIF are confirmed, and a correlation between their results is assessed in order to obtain a complete characterization of the analyzed samples.*

**Keywords:** time gated laser induced fluorescence spectroscopy, Raman spectroscopy, pigments, binders, principal component analysis.

**ПРИМЕНЕНИЕ СПЕКТРОСКОПИИ КОМБИНАЦИОННОГО РАССЕЯНИЯ СВЕТА И ЛАЗЕРНО-ИНДУЦИРОВАННОЙ ФЛЮОРЕСЦЕНТНОЙ СПЕКТРОСКОПИИ С ВРЕМЕННЫМ РАЗРЕШЕНИЕМ ДЛЯ ИДЕНТИФИКАЦИИ МАТЕРИАЛОВ, ИСПОЛЬЗУЕМЫХ В ЖИВОПИСИ**

**M. Romani<sup>1\*</sup>, S. Almaviva<sup>2</sup>, F. Colao<sup>2</sup>, R. Fantoni<sup>2</sup>, M. Marinelli<sup>1</sup>,  
A. Pasqualucci<sup>1</sup>, A. Puiu<sup>2</sup>, G. Verona-Rinati<sup>1</sup>**

УДК 535.375.5;535.372

<sup>1</sup> Национальный институт ядерной физики, Департамент промышленного машиностроения  
00133, Рим, Виа дель Политекнико, 1, Италия; e-mail: [martina.romani@uniroma2.it](mailto:martina.romani@uniroma2.it)

<sup>2</sup> Итальянское национальное агентство новых технологий, 00044, Рим, Италия

(Поступила 18 января 2018)

*Для определения характеристик материалов, применяемых в живописи, предложено использовать КР и лазерно-индуцированную флуоресцентную спектроскопию с временным разрешением. Взаимодополняющие возможности предлагаемых методов исследованы на наборе лабораторных образцов, имитирующих реальные произведения искусства. Полученные результаты подтвердили способность КР-спектроскопии определять характеристики пигментов и красителей. Однако идентификация связующих и защитных материалов оказалась затрудненной из-за их интенсивной*

\* This study was presented as an oral presentation during the conference “TECHNART 2017. Non-Destructive and Microanalytical Techniques in Art and Cultural Heritage”, Bilbao, May 2–6, 2017.

\*\* Full text is published in JAS V. 86, No. 2 (<http://springer.com/10812>) and in electronic version of ZhPS V. 86, No. 2 ([http://www.elibrary.ru/title\\_about.asp?id=7318](http://www.elibrary.ru/title_about.asp?id=7318); [sales@elibrary.ru](mailto:sales@elibrary.ru)).

флуоресценции. По этой причине анализируемые образцы также исследованы с помощью метода лазерно-индуцированной флуоресцентной спектроскопии с временным разрешением и классифицированы по характерным длинам волн излучения и временам распада. Подтверждены взаимодополняющие возможности рассматриваемых методов для получения полной характеристики анализируемых образцов и оценена корреляция их результатов.

**Ключевые слова:** лазерно-индуцированная флуоресцентная спектроскопия с временным разрешением, спектроскопия комбинационного рассеяния света, пигменты, связующие, метод главных компонент.

**Introduction.** During the last part of the 20th century, the growth of interest in the characterization and conservation of cultural heritage (CH) surfaces promoted the development of several diagnostic techniques addressed to solve conservation problems related to artwork materials [1, 2]. Polychrome surfaces (paints, frescoes, etc.) usually consist of many different constituents including pigments, binders, and protective materials, with a large variety of natural and synthetic compounds used by the artists in different historical periods. Therefore, the utilization of a single diagnostic analysis is often not sufficient to identify all the materials forming a painted layer; instead the integration of several techniques is highly recommended in most cases [3, 4]. In the field of CH, Raman, and laser induced fluorescence (LIF) spectroscopies are routinely employed for the characterization of painted surfaces, the former providing the “fingerprint” of several compounds [5–7], and the latter detecting the spectral signatures of luminescent materials [8–11]. In addition, the implementation of the time gated-LIF (TG-LIF), consisting in a time dependent measurement of the intensity over a defined period after the laser pulse, allows for associating to every observed emission a specific decay time [12, 13]. In this way a very detailed characterization of the surface under investigation can be obtained. Both TG-LIF and Raman techniques show the common advantage of being nondestructive combined with the capability to work *in situ* [14]. Indeed, the TG-LIF instrument used in this work is able to scan large surface (frescoes, etc.) at a distance up to 25 m in order to guide further localized spectroscopic analyses. As for the Raman system, it allows one to work in two different operation modes, within a laboratory setup inside a microscope and through a fiber optic probe for *in situ* measurements [7, 15, 16]. Nevertheless, besides all the peculiar advantages of both Raman and TG-LIF techniques, several issues could limit their capability to identify painted materials. For example, not all pigments and binders have a peculiar Raman spectrum. In addition, the occurrence of fluorescence phenomena could prevent the readability of the Raman signals [14]. On the other hand, the interpretation of TG-LIF spectra is not always straightforward, since a comprehensive database of binders, protective materials, and pigments, commonly used in the artistic field, is still missing [17, 18]. Therefore, the aim of this work consists of testing the complementary diagnostic capabilities of Raman and TG-LIF, aimed at the identification of artwork materials. For this purpose, more than 290 samples were realized using several combinations of pigments and binders commonly employed in modern and contemporary artworks, and then analyzed by Raman and TG-LIF. Significant correlation was obtained for the recognition of most materials in different substrates. This implies that the build-up of a combined references dataset is feasible and suitable for use as a reference for the characterization of painted surfaces by the two above-mentioned techniques.

**Materials and methods.** With the aim to build up a consistent spectral reference data, eight palettes of several pigments and dyes were prepared, employing different binders and resulting in 297 samples, as reported in Fig. 1a [19, 20]. In order to simulate the painting techniques of artists, two different preparatory layers of titanium and zinc whites were realized for each palettes [21]. Moreover, a column with no preparatory layer was also added for evaluating the spectral influence of the white preparations (Fig. 1b).

The pigments and binders analyzed in this work are listed in Tables 1 and 2, and grouped according to their chemical classification.

Raman spectra are recorded by using a portable instrument *i*-Raman (B&W TEK Inc., USA) equipped with a solid-state diode laser (GaAlAs) at 785 nm. The CCD detector is thermoelectrically cooled at 10°C. The resolution of the spectrometer is about 3 cm<sup>-1</sup> and covers the spectral range of wavelength shift between 75–3200 cm<sup>-1</sup>. By using a flexible fiber optic probe (1 m long), it is possible to focus the laser beam onto a spot down to 90 μm in diameter, while the reflected (Rayleigh) radiation is rejected through a notch filter. In order to optimize the signal and to avoid undesired burning phenomena, it is possible to set the laser power between 3–300 mW. In this work, except for the binders analysis, the laser power is kept well below the damage thresholds according to literature data and laboratory tests previously published in literature [22, 23].

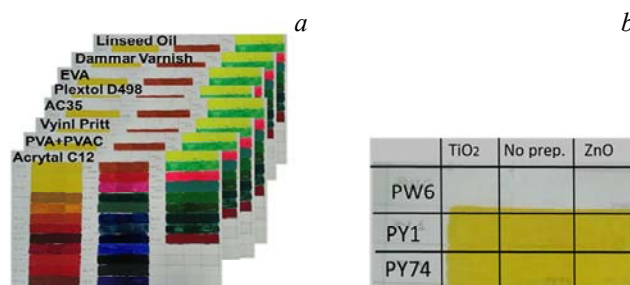


Fig. 1. a) Palettes of 35 pigments and dyes. For each binder a dedicated palette was realized by using the same pigments. b) Detail of a palette: the pigment samples are realized using three different preparatory layers: Titanium White (first column), without a preparatory layer (second column), and Zinc White (third column). (N.B. black lines are an artifact for eye guidance to distinguish different sample/preparation combination).

The LIF system used in this work is developed and patented at the laboratory ENEA of Frascati (Frascati-Rome, Italy) [22] and is capable to collect hyperspectral fluorescence images, scanning large areas. It is equipped with an Nd:YAG laser at 266 nm as excitation source with an energy of 1.5 mJ. The laser pulse duration is about 8 ns, operating at a maximum frequency of 20 Hz. A spectrometer (Jobin-Yvon CP240) allows collecting the light in the range of 190–800 nm with a spectral resolution  $\approx 2$  nm. The laser spot, being originally circular, is focused on the target by a quartz cylindrical lens, resulting in a linear blade of light, allowing scanning linear sections of the target instead of single points. The field of view is  $5.7^\circ$ , which means a linear scan 10 cm long at a distance of 1 m. The ICCD detector is an ANDOR iStar DH734 with squared pixels ( $1024 \times 1024$  pixels  $13 \times 13 \mu\text{m}^2$  each), mounted behind a slit parallel to the laser line footprint during the scanning. An image of  $1.5 \times 5 \text{ m}^2$  can be scanned in less than 2 min at 25 m distance (spatial resolution 2 mm). The TG-LIF measurements reported in this study occur on the nanosecond scale and are spectrally resolved in the full spectral bandwidth. In particular, they are implemented by modulating the trigger signal of the CCD intensifier, defining the camera gating delay time and the duration of the exposure. Therefore, the acquired LIF signal is spectrally resolved and time integrated in the previously defined gate. In order to record the decay time of the investigated compounds, five different spectra are acquired at different delays from the laser pulse (0, 10, 20, and 30 ns) with a gate duration of 10 ns. This gate duration was chosen because it is slightly longer than the laser pulse; on the other hand, delays longer than 40 ns were not considered because for all the observed samples no later signal was detected. The above-mentioned experimental settings do not allow estimating the decay times equal to or lower than the laser pulse (8 ns); therefore this study is limited to the characterization of components with longer decays. In addition, the time-gated characterization of pigments is only qualitative, and the spectral position of the band with the slowest decay time is given.

**Results and discussion. Pigments analysis.** The main Raman peaks and TG-LIF spectral features of the investigated samples are reported in Table 1. Specifically, the names of the analyzed pigments are listed in the first column, the main Raman peaks in the second one, while the TG-LIF emission bands acquired with no delay and with 20 ns delay in the third and fourth ones, respectively.

The Raman spectra were recorded in the so-called “fingerprint” region ( $100\text{--}1800 \text{ cm}^{-1}$  Raman shift), which is the typical range where the most significant Raman features are present, whereas features above  $1800 \text{ cm}^{-1}$  are generally weaker [23]. An exception was observed for the pigment PB27 (Prussian blue), whose main Raman peak is found at about  $2100 \text{ cm}^{-1}$ , according to data published in [24]. More than 80% of the analyzed pigments exhibit a set of characteristic Raman peaks consistent with literature data [25], proving the match between pigment commercial labels and their composition. However, the spectral position and the intensity may vary slightly from the literature, depending on the use of different instrument (e.g., spectral calibration). It is worth noting that some pigments (Pbk7, Pbk10, PB16, PR122, and PV23) are characterized by very weak Raman signal intensity. Indeed, such pigments can be better characterized using different excitation wavelength [21]. It should be pointed out that no changes in pigment spectra were detected when they are dispersed in different binders.

TABLE 1. Raman and TG-LIF Results (nm) from the Analyzed Pigments and Dyes

Pigment	Main Raman peaks	TG-LIF (no delay)	TG-LIF (20 ns delay)
<i>Phthalocyanines</i>			
PB15	255w, 481m, 591s, 677w, 744s, 830w, 947w, 1100w, 1141m, 1183w, 1212w, 1299w, 1331m, 1440m, <b>1514s</b>	N/A	N/A
PG7	685s, <b>737s</b> , 775s, 814w, 1083m, 1212m, 1281m, 1339m, <b>1530s</b>	N/A	N/A
PG36	322w, 662m, <b>747s</b> , 1164w, 1195w, 1267m, 1320m, 1530s	600	600
<i>Azo compounds</i>			
PY1	183w, 360w, 399w, 619w, 642w, 801w, 1086m, 1262s, <b>1326s</b> , 1350m, 1402m, 1489w, 1505w, 1591s	520	520
PY74	155w, 278m, <b>1082s</b> , 1260m, 1326m, 1354w, 1502w, 1591w	520	520
PY110	<b>171s</b> , 385w, 452m, 549m, 591w, 621w, 681m, 723m, 782w, 830w, 926w, 1164s, 1199w, 1229s, 1314w, 1378w, 1549w, 1666s, 1717w	520	N/A
PY151	136w, 197w, 378m, 610w, 949w, 1021w, 1143s, 1197m, 1247s, <b>1385s</b> , 1453w, 1494w, 1512w, 1578s, 1601m, 1652w	520	520
PR3	340s, 381w, 455m, 501w, 614s, 721m, 795s, 842m, 922w, 985s, 1074w, 1125s, 1183s, 1214m, 1205w, 1320s, <b>1331s</b> , 1394m, 1446m, 1494m, 1553w, 1605w, 1620m	550–650	N/A
PR49	301w, 344w, 410w, 457m, 640w, 719m, <b>987s</b> , 1035w, 1096, 1206s, 1224m, 1350m, 1405wm, 1424ww, 1465w, 1428w, 1552w, 1608w	600	N/A
PR146	630w, <b>955s</b> , 1265w, 1279w, 1354m, 1425w, 1498s, 1575s	600	N/A
PO5	223w, 387w, 625w, 836w, 983w, 1316m, <b>1341s</b> , 1402w, 1446m, 1608m	N/A	N/A
PG8	313m, 351w, 378w, 443s, 472s, 490m, 534s, 617m, 634s, 666s, <b>749s</b> , 877s, 1021m, 1057w, 1149w, 1254w, 1352, 1467w, 1503w, 1583w	N/A	N/A
<i>Ocher</i>			
PR102	146w, 223m, <b>290s</b> , 405w, 608w	600	N/A
PY43	141w, 308m, <b>401s</b> , 551m	N/A	N/A
<i>Diketopyrrolopyrrole (DPP)</i>			
PR254	<b>127s</b> , 190w, 271w, 349m, 450w, 521w, 621m, 640w, 685s, 723m, 926m, 1051s, 1088w, 1199w, 1254w, 1305w, 1324s, 1400w, 1440w, 1496w, 1522m, 1575s, 1592s, 1664w	600–700	N/A
PR255	<b>103s</b> , 164w, 232w, 248m, 317s, 494m, 610w, 638w, 675m, 692m, 930m, 999s, 1029m, 1051m, 1162w, 1206w, 1264w, 1307m, 1322m, 1344s, 1418w, 1560s, 1586s, 1601s, 1659w	600–700	N/A
<i>Perylene</i>			
PR224	387w, 534w, 1049w, <b>1309s</b> , 1380m, 1575w, 1592w	600–700	600–700
<i>Quinacridone</i>			
PR 122	N/A	600–700	600–700
<i>White</i>			
PW4	<b>437s</b> , 595w, 809m, 838m, 1301w, 1449s, 1733w	400–500	400–500
PW6	143w, 230m, <b>443s</b> , 606s, 803w, 834w, 1451w	380 nm	380 nm
<i>Ultramarine</i>			
PB27	<b>274s</b> , 525s, 2135m	N/A	N/A
<i>Hexacyanoferrate</i>			
PB29	<b>548s</b>	N/A	N/A
<i>Dioxazine</i>			
PV 23	N/A	N/A	N/A
<i>Fluorescent</i>			
Pink	N/A	N/A	N/A
Yellow	N/A	N/A	N/A
Green	N/A	N/A	N/A

Continue Table 1

Pigment	Main Raman peaks	TG-LIF (no delay)	TG-LIF (20 ns delay)
<i>Chromium Oxide</i>			
PG17	290w, 351m, <b>552s</b> , 610m	600	N/A
	Black		
PBk7	N/A	N/A	N/A
PBk10	N/A	N/A	N/A

Notes (strong), m (medium) or w (weak), while the most intense peak are in bold; N/A (not available).

In contrast to the Raman results providing the identification of the majority of the analyzed pigments, the analysis of the TG-LIF results may be not straightforward (see Table 1). The assignment of a spectral emission to a specific compound may require an accurate post-processing procedure. In addition, it should be noted that a real artwork surface characterization can be affected by different factors, such as aging, exposure to chemicals, and interaction with different types of supports (plaster, wood, canvas, etc.), possibly modifying their spectral response with respect to that of the laboratory samples [16]. In this study, we ruled out the problem considering the low penetration capability of UV excitation beam and adopting appropriate post-processing data, as for example the principal component analysis, which allows isolating the spectral behaviors of the painting materials, intentionally avoiding other undesirable contributions (support, protective materials, etc.) [11–13]. However, most of the pigments/dyes analyzed in this work did not show any peculiar emission band, possibly leading to an unambiguous identification. For example, it was observed that from the obtained LIF spectra it is not always possible to discriminate among pigments characterized by the same color (see Table 1). Indeed, all the red pigments showed a prominent band between 600–650 nm.

On the other hand, all the azo yellow pigments are characterized by an emission band at 520 nm, which was not observed in other yellow pigments (e.g., PY43). This implies that it is possible to discriminate among yellow pigments belonging to different classes, but, in vice versa, it makes it very difficult to distinguish ones of the same class. To better clarify this issues, spatially averaged fluorescence spectra (i.e. 528 spectra) obtained on the yellow azo-pigment PY74, mixed with an acrylic binder (Primal AC35), are reported in Fig. 2a. The spectra were acquired on three different preparatory layers: titanium white (blue line), without a preparatory layer (red line), and zinc white (black line). In all the acquired spectra five main emission bands are recognizable; the first one peaked at 290–300 nm, the second between 330–350 nm, the third at 380 nm, another between 400–450 nm, and the last at 510–550 nm. It should be noted that, even if the sample preparations are dissimilar, the acquired spectra are differentiated from each other only by the relative intensities of the aforementioned emission bands. Then, considering the relative intensity as a parameter of the concentration, it is possible to suppose that the spectra acquired on the two preparatory layers (black and blue lines) are characterized by a higher concentration of zinc white (380 nm) [18] and titanium white (400–450 nm) [18]. At this point, in order to extract the relevant features from spectra belonging to the hy-

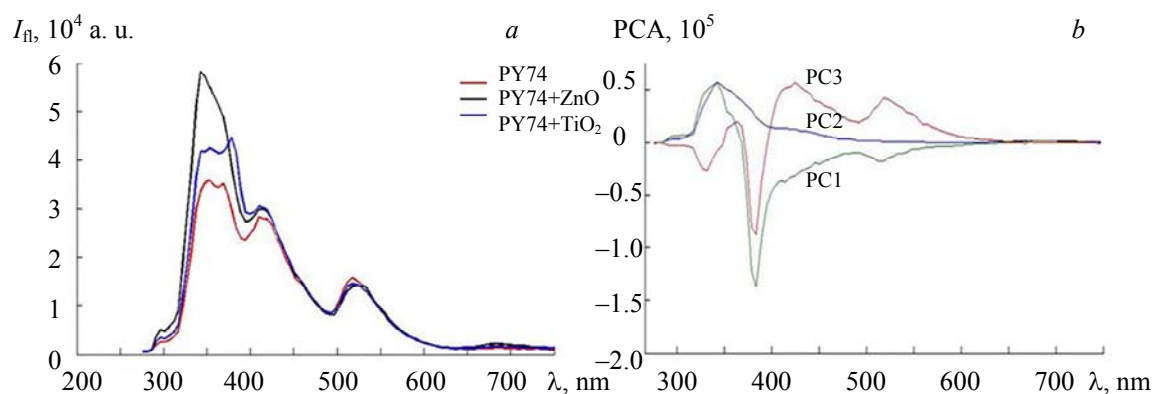


Fig. 2. a) LIF spectrum of PY74 in three different configurations: the pigment without a preparatory layer (red line) and with Zinc white (black line) or Titanium white (blue line) used as substrates. b) PCA analysis of PY74: the first three components are acquired at 0 ns delay.

perspectival image (>800 point of measure of PY74 on three different preparatory layers), the Principal Component (PC) analysis was used [16]. Although, it is commonly accepted that the PC loadings do not possess a direct physical meaning, they can nevertheless be described in terms of bands. Specifically, in some cases, a given PC loading could be well defined by spectroscopic bands with associated peaks, while in other cases complicated trends are observed, with the combination of positive and negative peaks. Usually a small number of PC loading (typically from 3 to 8 components) is enough to describe the entire spectral data set [16]. In this case, we chose to reduce our data to the first three components, as reported in Fig. 2b. The first PC loading (PC1, blue line) is characterized by two shoulders between 290–300 and 330–350 nm, probably ascribed to the acrylic binder Primal AC35, as reported in [26]. The second one (PC2, green line) is characterized by an emission at 370–380 nm related to the zinc white [18], and finally the third loading (PC3, red line) showed an emission between 400–500 nm, due to the titanium white [18]. In addition, in the PC3 loading, a further band at 520 nm is also observed, probably assignable to the pigment PY74. However, as previously described, the majority of the analyzed yellow pigments is characterized by this emission, producing a substantial ambiguity in their identification, when only LIF analysis is considered. For this reasons, the fluorescence data must be integrated with the ones acquired by Raman. Indeed, it was proved, that the Raman analysis is able to operate a univocal identification of all the analyzed azo-pigments, as shown in Table 1. It should be mentioned though that both Raman and TG-LIF spectroscopy proved to be unable to characterize fluorescent pigments (pink, green, and yellow). The strong fluorescence background observed in these cases adversely affects the Raman analysis, while the high fluorescence yield makes the TG-LIF spectra prone to saturation, causing strong spectral distortions. Therefore, this approach does not seem suitable for the identification of such type of compounds.

*Preparation layers analysis.* As previously described, the PC analysis demonstrated its capability to extract from a hyperspectral image the contribution arising from the white pigments used as preparatory layers. In order to evaluate the potentiality of the Raman technique to extract information on the preparatory layer, the results obtained on the pigment PR3 mixed with the dammar varnish on the three substrate preparations (i.e., TiO<sub>2</sub>, ZnO, and no preparatory layer) are shown in Fig. 3. The Raman spectra for the three samples are shown in Fig 3b. The 437 cm<sup>-1</sup> peak of the zinc white result is undetectable in the Raman spectrum of PR3 on ZnO (red line), probably due to its weak intensity [24], thus not allowing the identification of the preparatory layer pigment. On the contrary, a qualitative evaluation of the contribution of the Titanium white (black line) is possible due to its strong peaks at 443 and 606 cm<sup>-1</sup>, which spectrally interferes with the ones characteristic of PR3 at 455 and 614 cm<sup>-1</sup> (blue line). The LIF spectra of PR3 are reported in Fig. 3c. In contrast to those observed in the Raman ones, the spectral features of the Zinc white are clearly detectable thanks to its characteristic emission wavelength at 380 nm (Fig. 3c, blue line). On the contrary, the characteristic emission

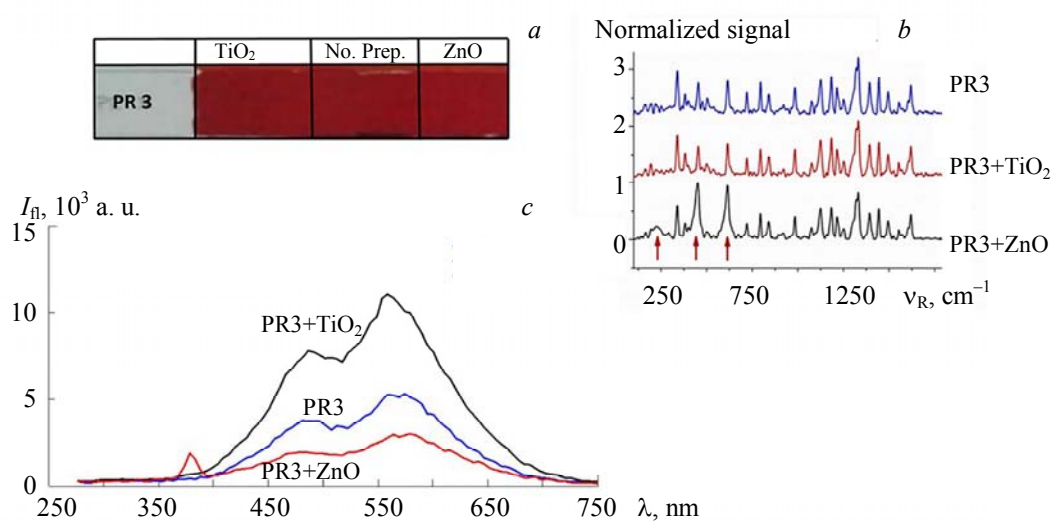


Fig. 3. (a) Detail of sample palettes of the PR3 pigment. (b) Raman spectra of PR3 without preparatory layer (blue line), with an underlying preparatory layer of ZnO (red line) and TiO<sub>2</sub> (black line). The red arrows highlight the contribution of TiO<sub>2</sub> to the PR3 spectrum. (c) LIF spectra of PR3 and Titanium white (black line) and Zinc white (blue line) as preparatory layers.

of Titanium white between 400–450 nm is superimposed on that of PR3, making difficult the identification of such a preparatory layer (Fig. 3c, black line). Therefore, considering the complementary information obtained by Raman and TG-LIF their, integration is highly recommended for an unambiguous characterization of the white preparation layer.

**Raman binders analysis.** In previous works, the authors studied the spectral features and decay times of the binders used in this study by reporting a classification through a TG-LIF analysis [17, 26]. Figure 4a shows the LIF spectra acquired with no delay from the laser pulse of the analyzed binders, except for the linseed oil and dammar varnish not reported here: each analyzed binder is characterized by a peculiar LIF spectrum. Moreover, the invasiveness of UV radiation and its potential damaging has been investigated by observing the samples with an optical microscopy and measuring the colorimetric coordinates after each TG-LIF acquisitions. No evidence of damage effects related to laser irradiation were observed, nor any change in color by comparing the colorimetric coordinates before and after exposure to the UV laser radiation. A detailed characterization by Raman was thus performed in order to achieve complementary information to support the TG-LIF results. Due to the difficulties in identifying the binders, especially when they are mixed with the pigments, they were measured as pure compounds layered on a black paper. In addition, the laser power was increased by a factor of 12 with respect to the one used for the pigment analysis in order to get a significant signal-to-noise ratio. In Fig. 4b, the spectra of seven different media are shown. The spectrum of linseed oil is not reported due to its intense and unstructured background, which made it difficult to optimize the acquisition parameters. The arrows mark the spectral differences related to the analyzed binders [27]. It is worth pointing out that many of the recorded spectra do not show significant contributions for their identification. To evaluate the possibility of an automatic discrimination of different binders by Raman spectra, PCA on the spectral emissions was performed and the results reported in Fig. 4c. The graph shows that only the vinyl binders are well discriminated from the substrate (green points in Fig. 4c), thanks to the main contribution of their characteristic peaks at  $619\text{ cm}^{-1}$ . On the other hand, the binders grouped in the red circle (Acrytal C12, Plextol D498) are slightly displaced with respect to the support with a larger dispersion, but enough to be differentiated from the substrate. Instead, dammar varnish (blue circle) is the only one strongly transparent to Raman, and its spectra are partially superimposed with the ones of the substrate, so that the

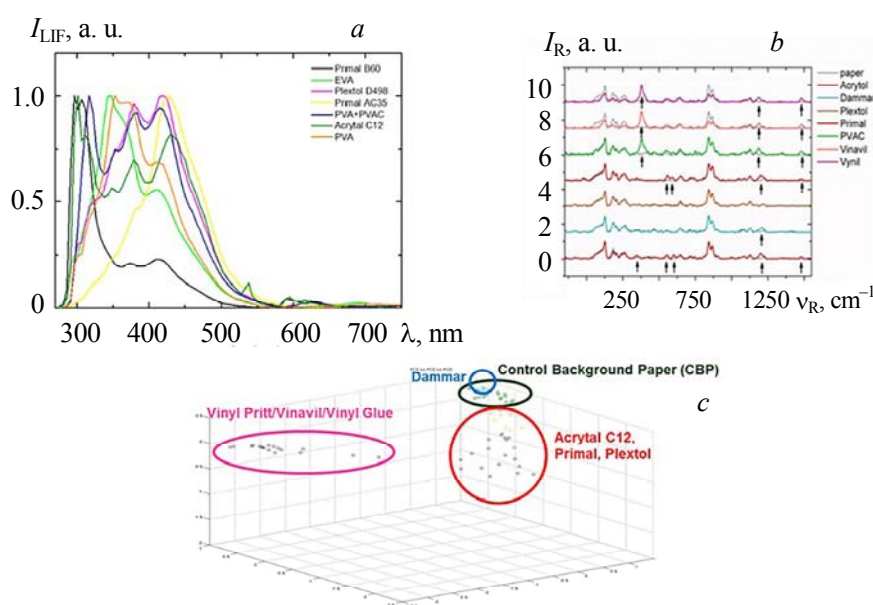


Fig. 4. a) LIF spectra of the analyzed binders acquired with no delay from the laser pulse. The spectra of linseed oil and dammar varnish are not shown because they have no characteristic LIF spectra. b) Raman spectra of different binders on paper obtained at a laser power of 240 mW and an integration time of 15 s. Background contribution is subtracted and the spectra are normalized and shifted along the y axis.

The spectrum of the substrate is shown in light gray for each binder. The arrows mark the spectral features specific to each binder. c) PCA analysis of Raman spectra of the analyzed binders

TABLE 2. Raman Peaks ( $\text{cm}^{-1}$ ) of Binder References

Binders		Raman Peaks
Acrylic	Primal B60	364, 485, 595, 805, 854, 990, 1111, 1452, 1727
	Primal AC 35	278, 360, 485, 597, 809, 842, 962, 1060, 119, <b>1295</b> , 1449, 1731
	Acrytal C12	365, 599, 807, 856, 1449, 1725
	Plextol D498	273, 358, 485, 595, 807, 842, 985, 1058, 1119, 1296, 1451, 1727
Vinyl	EVA	367, <b>630</b> , 821, 882, 1020, 1123, 1353, <b>1436</b> , <b>1729</b>
	PVA+PVAC	362, <b>630</b> , 838, 1000, 1121, <b>1434</b> , <b>1734</b>
	PVA	362, <b>630</b> , 815, 886, 1016, 1116, 1354, <b>1442</b> , <b>1733</b>
Natural	Linseed oil	No characteristic Raman spectrum
	Dammar	No characteristic Raman spectrum

PCA was not able to completely separate their contributions. It should be pointed out that the high laser power used here for the binder's identification is not suitable for real artworks, where the use of lower laser power is mandatory in order to avoid risk of damage. This problem can be overcome by using a higher sensitivity instrumental setup, which is presently under development.

**Conclusion.** The results obtained here demonstrated that Raman and TG-LIF are complementary diagnostic techniques for the study of polychrome surfaces. Specifically, this study on a set of ancient and contemporary pigments demonstrates how Raman spectroscopy is a suitable tool for identifying pigments and dyes. Indeed, for more than the 80% of the investigated pigments, a characteristic spectrum was obtained, comparable to the data available in the literature. However, the possibility to use multiple laser wavelengths in portable instruments would improve such a result, allowing an increased number of identifiable pigments, both directly and by crossing data from multiple laser excitations. As for the TG-LIF spectroscopy, the analyzed samples were classified through the study of their characteristic emission wavelengths and decay times. The interpretation of TG-LIF spectra is not always straightforward, since a comprehensive reference data collection of materials commonly used in the artistic field is still missing. At present, an integration with Raman results is therefore highly recommended. The contribution of the preparatory layers in the pigments samples was also studied. From the current experimental results it comes out that Raman analysis is not always suitable to characterize the preparation layer, especially when it is realized by using ZnO. In this specific case, integration with the LIF analysis is very useful for layer identification. Finally, the characterization of binders by Raman spectroscopy was carried out in order to complete the TG-LIF results already achieved by the authors in previous works. The contribution from the binding media in the Raman spectra is generally negligible, being that the spectral features of these compounds are very weak as compared to the ones originating by pigments and dyes. In conclusion, the complementary diagnostic capabilities of Raman and TG-LIF aimed at the identification of artwork materials was tested. The integration of such techniques in the analysis of painted layers is highly recommended in order to overcome the disadvantages commonly affecting either of them separately. All Raman and TG-LIF data acquired in this work were summarized in a reference spectral data collection useful for the characterization of painted surfaces.

**Acknowledgment.** Latium Region is gratefully acknowledged for funding the COBRA project "Sviluppo e diffusione di metodi, tecnologie e strumenti avanzati per la Conservazione dei Beni culturali, basati sull'applicazione di Radiazioni e di tecnologie Abilitanti" (Ir 13/2008, project No. 1031).

## REFERENCES

1. G. Bitossi, R. Giorgi, M. Mauro, B. Salvadori, L. Dei, *Appl. Spectrosc. Rev.*, **40**, No. 3, 187–228 (2005).
2. G. Artioli, *Scientific Methods and Cultural Heritage: an Introduction to the Application of Materials Science to Archaeometry and Conservation Science*, Oxford, Oxford University Press (2010).
3. A. Deneckere, M. De Reub, M. P. J. Martens, K. De Coened, B. Vekemans, L. Vinczea, De Maeyer, P. Vandenabeele, L. Moensa, *Spectrochim. Acta A*, **80**, No. 1, 125–132 (2011).
4. C. Ricci, I. Borgia, B. G. Brunetti, C. Miliani, A. Sgamellotti, C. Seccaroni, P. Passalacqua, *J. Raman. Spectrosc.*, **35**, No. 8-9, 616–621 (2004).
5. I. M. Bell, J. H. Clark, P. J. Gibbs, *Spectrochim. Acta A*, **53**, No. 12, 2159–2179 (1997).
6. G. Burrafato, M. Calabrese, A. Cosentino, A. M. Gueli, S. O. Troja, A. Zuccarello, *J. Raman. Spectrosc.*, **35**, No. 10, 879–886 (2004).



7. P. Vandenabeele, B. Wehling, L. Moens, H. Edwards, M. De Reu, G. Van Hooydonk, *Anal. Chim. Acta*, **407**, No. 1-2, 261–274 (2000).
8. A. Nevin, G. Spoto, D. Anglos, *Appl. Phys. A: Mater.*, **106**, No. 2, 339–361 (2012).
9. D. Anglos, M. Solomidou, I. Zergioti, V. Zaffiropulos, T. G. Papazoglou and C. Fotakis., *Appl. Spectrosc.*, **50**, 1331–1334 (1996).
10. T. Miyoshi, Y. Matasuda, *Jpn. J. Appl. Phys.*, **26**, No. 2, 239–245 (1987).
11. R. Fantoni, L. Caneve, F. Colao, L. Fiorani, A. Palucci, R. Dell’Erba, V. Fassina, *J. Cult. Herit.*, **14**, No. 3, 59–65 (2013).
12. A. Cesaratto, C. D’Andrea, A. Nevin, G. Valentini, F. Tassone, R. Alberti, T. Frizzi, D. Comelli, *Anal. Methods*, **6**, 130–138 (2014).
13. A. Nevin, D. Comelli, G. Valentini, D. Anglos, A. Burnstock, S. Cather, R. Cubeddu, *Anal. Bioanal. Chem.*, **388**, No. 8, 1897–1905 (2007).
14. A. P. Shreve, N. J. Cherepy, R. A. Mathies, *Appl. Spectrosc.*, **46**, No. 4, 707–711 (1992).
15. R. A. Goodall, J. Hall, H. G. M. Edwards, R. J. Sharer, R. Viel, P. M. Fredericks, *J. Archaeol. Sci.*, **34**, 666–673 (2007).
16. M. Romani, F. Colao, R. Fantoni, M. Guiso, M. L. Santarelli, *J. Appl. Laser Spectrosc.*, **1**, 29–36 (2014).
17. M. Marinelli, A. Pasqualucci, M. Romani, G. Verona-Rinati, *J. Cult. Herit.*, **23**, 98–105 (2017).
18. I. Borgia, R. Fantoni, C. Flamini, T. M. Di Palma, A. Giardini Guidoni, A. Mele, *Appl. Surf. Sci.*, **127-128**, 95–100 (1998).
19. F. N. Jones, W. Mao, P. D. Ziemer, F. Xiao, J. Hayes, M. Golden, *Prog. Org. Coat.*, **52**, No. 1, 9–20 (2005).
20. P. Seymour, *The Artist’s Handbook*, Arcturus Publishing Limited, London (2003).
21. M. Bacci, M. Picollo, G. Trumpy, M. Tsukada, D. Kunzelman, *J. Am. Inst. Conserv.*, **46**, No. 1, 27–37 (2007).
22. L. Fiorani, L. Caneve, F. Colao, R. Fantoni, P. Ortiz, M. A. Gómez, M. A. Vázquez, *Adv. Mater. Res.*, **133-134**, 253–258 (2010).
23. N. C. Scherrer, S. Zumbuhel, F. Delavy, A. Fritsch, R. Kuehnen, *Spectrochim. Acta A*, **73**, 505–524 (2009).
24. I. M. Bell, R. J. H. Clark, P. J. Gibbs, *Spectrochim. Acta. A*, **53A**, 2159–79 (1997).
25. M. C. Caggiani, A. Cosentino, A. Mangone, *Microchem. J.*, **129**, 123–132 (2016).
26. M. Romani, M. Marinelli, A. Pasqualucci, G. Verona-Rinati, *Lasers in the Conservation of Artworks XI, Proc. Int. Conf. LACONA XI*, Kraków, Poland, 20–23 September 2016, NCU Press, Toruń (2017).
27. F. Pozzi, J. R. Lombardi, M. Leona, *Herit. Sci.*, **1**, 23 (2013).